ISSN 1028-334X, Doklady Earth Sciences, 2007, Vol. 415, No. 5, pp. 804–809. © Pleiades Publishing, Ltd., 2007.
Original Russian Text © A.E. Vershinin, I.I. Likhanov, V.V. Reverdatto, 2007, published in Doklady Akademii Nauk, 2007, Vol. 415, No. 2, pp. 230–235.

GEOCHEMISTRY

Geochemistry and Nature of the Protolith of Lower Proterozoic Fe–Al Metapelites in the Transangara Region, Yenisei Ridge

A. E. Vershinin, I. I. Likhanov, and Academician of the RAS V. V. Reverdatto

Received February 27, 2007

DOI: 10.1134/S1028334X07050327

Numerous facts and evidence in support of the essentially isochemical character of metamorphism opened wide the possibility for deciphering the primary nature of metamorphic rocks. One of the most efficient methods for reconstruction of the protolith and geodynamic settings of its formation is analysis of REE patterns and indicator ratios between other trace elements. These methods are widely applied in studying magmatic and sedimentary rocks, but less often used for metamorphic rocks because of a lack of data on the trace element distribution. Up to now, only limited data [1, 2] have been available on REE distribution in Fe–Al pelites, the metamorphism of which produces rare mineral assemblages of chloritoid, Fe-cordierite, and other minerals [3, 4]. According to published data, such a specific composition of the rocks is attributed to laterite weathering [5]. However, this conclusion is inconsistent with the frequent absence of a complete weathering crust profile in the Precambrian sequences [6], which stimulated great interest in the origin of these rocks. Therefore, our work is aimed at reconstruction of the composition and major features of the protolith based on new geochemical data on Fe–Al metapelites.

We used Lower Proterozoic regionally metamorphosed rocks of the Teya Group, which compose the Chapa anticline at the middle reaches of the Chapa River (Transangara region, Yenisei Ridge). The core of the anticline consists of quartzites and crystalline schists of the Karpinsky Ridge Formation (hereafter, Karpinsky Formation), while the limbs are composed of metaterrigenous–carbonate rocks of the Penchenga Formation (Fig. 1). The folded structure of the region is complicated by NW-trending thrust faults [7] ascribed to the Uvolzh'e fault zone in the northern sector of the Tatar deep fault. The most distal (relative to the thrust zone in the study area) low-pressure metapelites of the Penchenga and Karpinsky formations, which consist of the (Ms + Chl + Bt + Qtz + Pl) and (Ms + Bt + Qtz + And + St + Pl ± Grt ± Chl) mineral assemblages, respectively, formed under conditions of greenschist and epidote–amphibolite facies. Upon approaching the thrust fault, regional metamorphism was replaced by moderate-pressure collisional metamorphism of the kyanite–sillimanite type. A spatial transition from regionally metamorphosed low-pressure rocks to the higher pressure collision-related rocks is marked by the simultaneous appearance of kyanite and sillimanite. The limiting (Ms + Bt + Qtz + Ky + St + Grt + Pl + Sil) assemblage with relicts of andalusite appeared under conditions of the kyanite–staurolite subfacies of the kyanite schist facies. These rocks (4–5 km wide) are bounded on the east by a NW-trending thrust. The results of geothermobarometry and calculations of the *PT* path indicate a gradual increase in pressure with the approaching thrust: from the initial 4–5 kbar (metapelites of the Penchenga Formation) to 5.0–5.5 kbar (metapelites of the andalusite–sillimanite type, Karpinsky Formation) and up to 8.1–8.4 kbar (inner zone of kyanite blastomylonites of kyanite–sillimanite type) at an insignificant increase in temperature (from 620 to 710°C) [8].

The metapelite samples located at different distances from the thrust fault (Table 1) show the following compositional variations (wt %): SiO_2 58.29–61.03, CaO 0.23–0.96, Na_2O 0.24–0.93, and K_2O 2.28–3.34. The compositional variations of other components are less significant. The differences in contents of Si, Ca, Na, and K can be explained by the primary chemical heterogeneity of the rocks expressed in different modal contents of quartz, mica, and plagioclase. Relative to metapelites of the Karpinskii Formation, the metapelites of the Penchenga Formation are enriched in K_2O and depleted in Fe_2O_3. Despite some chemical heterogeneity, these rocks are classed with low-Ca (<1 wt %) and moderate-K_2O (2.3–3.3 wt %) metapelites simultaneously enriched in Fe and Al. They are characterized by elevated contents of total Fe and Al (Fig. 2a), but low contents of TiO_2, MgO, CaO, and Na_2O as compared to

Institute of Geology and Mineralogy, Siberian Division, Russian Academy of Sciences, pr. akademika Koptyuga 3, Novosibirsk, 630090 Russia; e-mail: likh@uiggm.nsc.ru

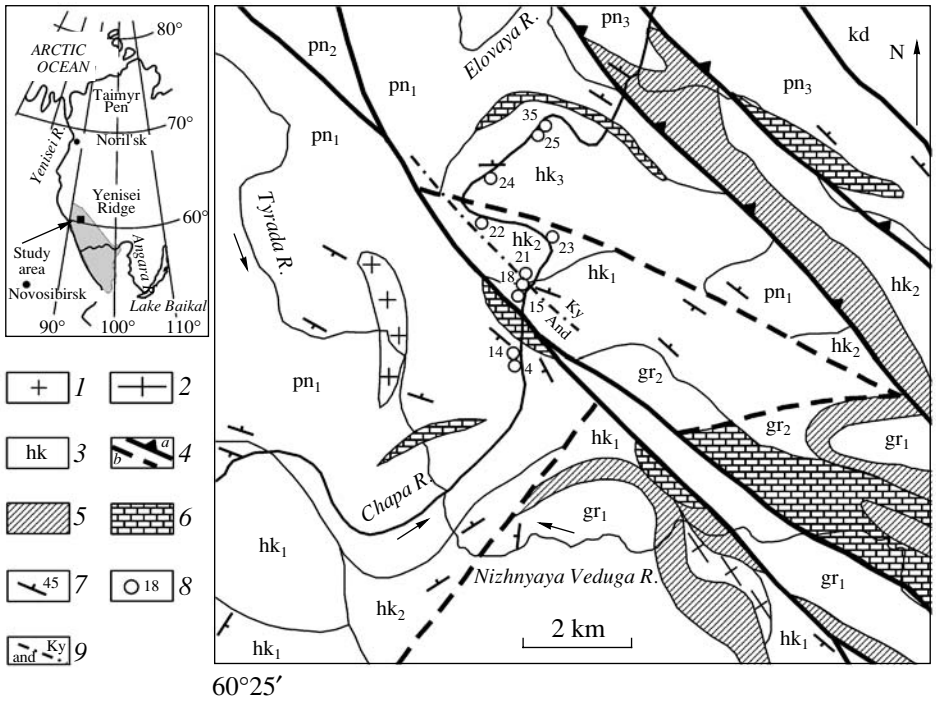

Fig. 1. Geological scheme of Precambrian crystalline metasedimentary rocks at middle reaches of the Chapa River. (*1*) Granites of the Teya Complex, (*2*) granite gneisses of the Garev Complex; (*3*) metasedimentary rocks: Lower Riphean (Korda Formation, Kd); Lower Proterozoic (Penchenga Formation: actinolite schists (pn_1), biotite schists (pn_2), graphite schists (pn_3); Karpinskii Formation: schists with quartzite and marble interlayers (hk_1), two-mica schists with staurolite and garnet (hk_2); undifferentiated Archean–Lower Proterozoic (Garev Formation: leucocratic gneisses (gr_1), quartzites and micaceous schists (gr_2)); (*4a, 4b*) thrusts (jags show dip direction) and subsidiary faults, respectively; (*5*) amphibolites; (*6*) marbles; (*7*) dip and strike; (*8*) sampling locality; (*9*) And–Ky isograd.

the average compositions of typical metapelites in the Postarchean Australian shales (PAAS) [9].

To reconstruct the composition, weathering conditions, and paleogeographic environment of sedimentation, we applied the petrochemical models and diagrams of Yudovich and Ketris [6] and Predovsky [10], as well as well-known petrochemical ratios, such as the chemical index of alteration CIA = $[Al_2O_3/Al_2O_3 + CaO + Na_2O + K_2O)] \cdot 100$, the chemical index of weathering CIW = $[Al_2O_3/Al_2O_3 + CaO + Na_2O)] \cdot 100$, the index of compositional variability (or the index of compositional maturity) IVC = $(Fe_2O_3 + K_2O + Na_2O + CaO + MgO + TiO_2)/Al_2O_3$, and the index of plagioclase alteration PIA = $[(Al_2O_3–K_2O)/(Al_2O_3 + CaO + Na_2O – K_2O)] \cdot 100$ (Table 1).

Based on similar values of hydrolyzate module HM = $(Al_2O_3 + TiO_2 + Fe_2O_{3tot} + MnO)/SiO_2$ within the range of 0.51–0.54, iron module IM = $(Fe_2O_{3tot} + MnO)/SiO_2$ equal to 0.32–0.39, aluminosilicate module AM = Al_2O_3/SiO_2 equal to 0.36–0.38, and femic module FM = $(Fe_2O_3 + MnO + MgO)/SiO_2$ equal to 0.15–0.19, the studied metapelites can be ascribed to normal- and supersiallites [6]. The values of alkalinity module AM = Na_2O/K_2O (0.10–0.33) and potassium module KM = K_2O/Al_2O (0.10–0.15) indicate that the primary pelitic deposits were dominated by hydromica and chlorite. However, in relationships used for discrimination of pelitic sediments, such as the FM–NAM diagram [6], where NAM (normalized alkalinity module) = $(Na_2O + K_2O)/Al_2O_3$, and the FAK diagram [10], these rocks are localized in the compositional field dominated by kaolinite, probably owing to the paleogeographic environment. When approaching the source area, kaolinite clays could be accumulated in a continental setting, while fine clayey chlorite–hydromica material was transferred into coastal parts of the marine basins. Low values of alkalinity (NAM module 0.12–0.17) in combination with low contents of MgO (<2.45 wt %) and elevated contents of K_2O (>2.28 wt %) indicate that the source areas contained K-rich granites and lacked a volcanogenic admixture of mafic composition. The values of the titanium module TM = TiO_2/Al_2O_3 (0.03–0.06) are typical of the rocks accumulated in the coastal shallow basins under humid conditions. This is consistent with lithofacies data [11].

The high CIA, CIW, and PIA values ranging from 82.9 to 95.7 indicate that these metapelites were formed from the redeposited weathering crusts in warm and humid settings. This conclusion is supported by data on the IVC index (<1), which attests to the erosion of more mature material and its transport to the sedimentation

Table 1. Chemical compositions (wt %), main petrochemical modules, and indices of representative samples of metapelites of the Teya Group

Sample no.	SiO_2	TiO_2	Al_2O_3	Fe_2O_3	MnO	MgO	CaO	Na_2O	K_2O	L.O.I.	Total
4	58.95	1.50	21.60	7.35	0.15	1.73	0.67	0.42	3.34	4.25	100.1
14	58.82	1.37	21.67	7.24	0.14	1.82	0.69	0.45	3.18	4.64	100.1
15	58.91	0.78	21.52	8.74	0.14	1.57	0.23	0.72	3.06	4.22	100.1
18	59.00	0.80	21.80	8.52	0.15	1.62	0.27	0.82	2.96	4.16	100.0
21	59.75	0.70	21.60	8.35	0.15	1.83	0.34	0.33	2.66	4.17	100.1
22	59.29	0.98	21.55	8.72	0.16	1.95	0.73	0.32	2.46	3.86	100.1
23	59.70	1.12	21.97	8.09	0.17	1.82	0.79	0.28	2.60	3.42	100.1
24	60.35	1.18	21.58	8.78	0.14	2.35	0.76	0.24	2.29	2.37	100.1
25	61.03	1.29	21.81	8.02	0.15	2.03	0.96	0.38	2.28	2.02	100.1
35	60.49	1.27	21.79	8.25	0.17	2.30	0.93	0.30	2.42	1.95	100.0

Sample no.	HM	AM	FM	KM	AM	NAM	IM	íå	CIA	CIW	IVC	PIA
4	0.52	0.37	0.15	0.15	0.13	0.17	0.32	0.07	82.98	95.20	0.69	94.4
14	0.51	0.37	0.15	0.15	0.14	0.17	0.32	0.06	83.38	95.00	0.68	94.2
15	0.53	0.37	0.18	0.14	0.24	0.18	0.40	0.04	84.29	95.77	0.70	95.1
18	0.53	0.37	0.17	0.14	0.28	0.17	0.38	0.04	84.33	95.24	0.69	94.5
21	0.51	0.36	0.17	0.12	0.12	0.14	0.38	0.03	86.64	96.99	0.66	96.6
22	0.53	0.36	0.18	0.11	0.13	0.13	0.39	0.05	85.99	95.35	0.70	94.8
23	0.52	0.37	0.17	0.12	0.11	0.13	0.36	0.05	85.69	95.36	0.67	94.7
24	0.52	0.36	0.18	0.11	0.10	0.12	0.39	0.06	86.77	95.57	0.72	95.1
25	0.51	0.36	0.16	0.10	0.17	0.12	0.35	0.06	85.76	94.21	0.69	93.6
35	0.52	0.36	0.17	0.11	0.12	0.12	0.37	0.06	85.65	94.66	0.71	94.0

Note: Total iron is given as Fe_2O_3. See the text for abbreviations of modules and indices.

area. Thus, the Fe–Al metapelites were initially redeposited and metamorphosed products of the Precambrian weathering crust of the kaolinite, rather than laterite, type, as was considered earlier [5]. The Early Proterozoic chemical weathering at the Yenisei Ridge did not reach the stage of intense lateritization with the formation of zones of final decomposition of aluminosilicates and was limited by the formation of weathering products of mainly kaolinite–chlorite–hydromica composition.

The main parameters of the REE distribution patterns are as follows: total REE; the $(LREE/HREE)_n$ ratio, which is interpreted as indicator of the paleoclimate; parameters $Eu/Eu^* = Eu_n/(Sm_n + Gd_n) \cdot 0.5$ and $Ce/Ce^* = Ce_n/(Ln_n + Pr_n) \cdot 0.5$ as indicators of sedimentation environment; the $(La/Yb)_n$ ratio as the slope of the REE distribution; and the $(Gd/Yb)_n$ ratio as an indicator of HREE depletion. The latter two parameters are mainly controlled by the composition of the source area and local tectonics [9]. Table 2 presents the contents of REE and trace elements, as well as values of some indicator ratios (La/Sc, Th/Sc, La/Th, Co/Th, Th/U), which provide insight into the composition and formation conditions of the protolith.

The chondrite-normalized REE distribution patterns for all studied samples (Fig. 3) show a negative Eu anomaly (Eu/Eu* 0.41–0.79) and significant negative slope. This is evident from elevated ratios of $(La/Yb)_n$ = 3.11–14.75, $(Gd/Yb)_n$ = 0.71–2.11, and $(LREE/HREE)_n$ = 1.89–4.56 (Table 2). These features are typical of Postarchean shales and related to the presence of eroded granitoid material in the detritus [9]. Despite similar shapes, as well as conjugate variations in REE contents and ratios, the REE patterns of the studied rocks are significantly differentiated. The low-pressure metapelites have high LREE and HREE contents with the total REE content within 210–335 ppm and maximum values of

$(La/Yb)_n$ = 10.57–15.20, $(Gd/Yb)_n$ = 1.05–2.11, and $(LREE/HREE)_n$ = 3.65–4.56. In contrast, the total REE content is 184 ppm, while the respective ratios are equal to 9.16, 1.34, and 3.27 in the PAAS [9]. The high-pressure collision-related metapelites are distinctly depleted in LREE and HREE (total REE content 78.92–157.1 ppm) relative to the metapelites of previous zones and PAAS. Consequently, the high-pressure metapelites have lowered values of $(La/Yb)_n$ = 3.11–8.42, $(Gd/Yb)_n$ = 0.71–1.03, and $(LREE/HREE)_n$ = 1.89–3.34. The conjugate variations of REE contents toward the thrust fault can be caused by local chemical heterogeneity of the primary protolith or variations in the modal composition of rocks in the course of mineral reactions owing to collisional metamorphism.

The contents of lithophile elements (Rb, Cs, Ba, Sr) in the studied metapelites are slightly lower than those in PAAS, unlike the contents of practically all HFSEs (Zr, Hf, Y, Ta, Th) except U (Table 2). The inheritance of the primary composition of the magmatic protolith is confirmed by the high positive linear correlation between contents of HFSEs (Zr, Hf, Y, Ta, Nb) (Table 2). As for transition metals, the metapelites have higher contents of Sc and lower contents of Co and Ni as compared to PAAS. The revealed regularities emphasize both the influence of sediment recycling and the predominance of weathered granitoids in the erosion area. This is seen from the Eu/Eu* ratio (<0.85) and the intensity of their weathering. The erosion of felsic material is also supported by the elevated contents of Th/Sc (0.77–1.26) and Th/U (5.33–18.5) ratios relative to the average PAAS composition. This conclusion is consistent with the presence of weathered granites in the basal horizons of the Karpinskii Formation. In the Eu/Eu*–$(Gd/Yb)_n$ diagram [12], the data points of metapelites are localized mainly in the field of Postarchean cratonic sediments (Fig. 2b). A similar conclusion also follows from the position of data points of these rocks in the $(La/Yb)_n$–Yb_n diagram [13], where they are concentrated in the field of Postarchean granitoids enriched in HREE and depleted in Co and Ni as compared to the Archean felsic magmatic rocks (Fig. 2c). In the Rb–(Y + Nb) discriminant diagram, these rocks fall into the boundary fields between island-arc and within-plate granites (Fig. 2d). Intrusive rocks with similar geochemical characteristics are typical of post-collisional geodynamic settings [14]. The variations of the Ce/Ce* ratio in metapelites from 0.68 to 1.40

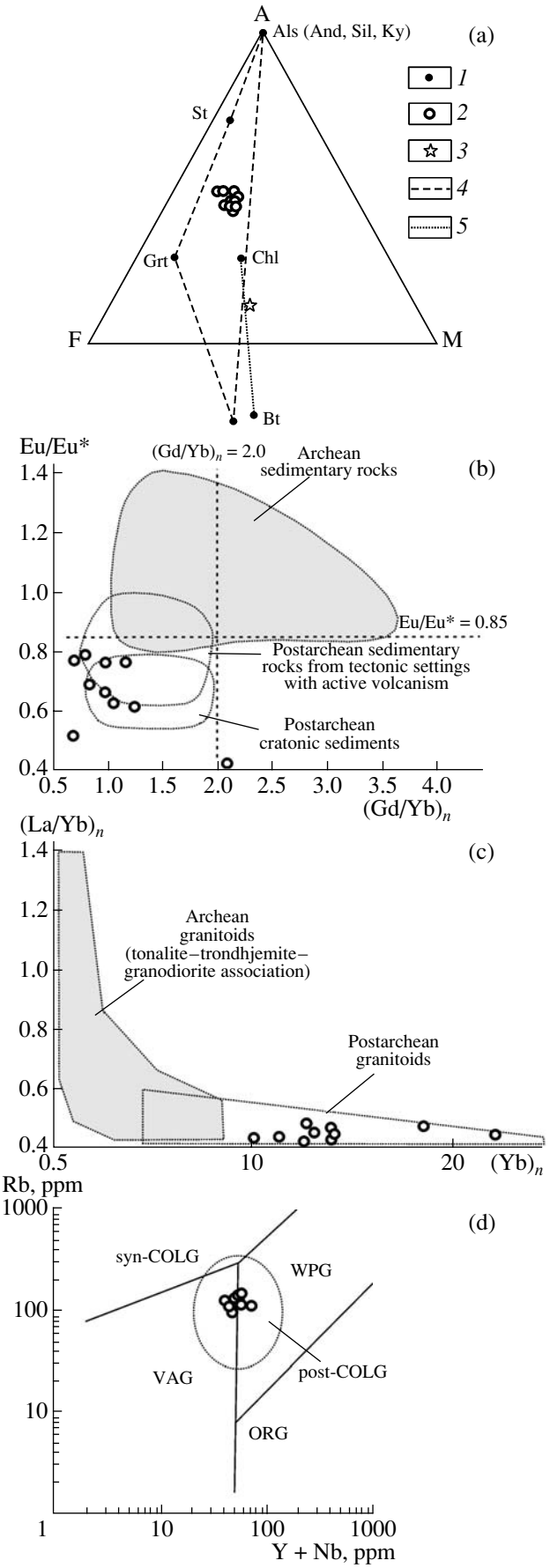

Fig. 2. Data points of metapelites of the Teya Group in various diagrams: (a) AFM, (b) Eu/Eu*–$(Gd/Yb)_n$, (c) $(La/Yb)_n$–Yb_n, (d) Rb–(Y + Nb). (*1*) Chemical composition of minerals; (*2*) chemical composition of metapelites; (*3*) average composition of typical metapelite; mineral assemblages of metapelites shown in Fig. 2a: (*4*) Karpinskii Formation, (*5*) Penchenga Formation. Compositional fields of granitoids shown in Fig. 2d: (post-COLG) postcollisional, (syn-COLG) collisional, (VAG) island-arc, (WPG) within-plate, (ORG) oceanic ridge.

Table 2. Contents of rare earth and trace elements (ppm) and their indicator ratios in metapelites of the Teya Group

Sample no.	La	Ce	Pr	Nd	Sm	Eu	Gd	Tb	Dy	Ho	Er	Tm	Yb	Lu
4	74	143	17.3	60	9.8	1.76	7.4	1.33	7.9	1.7	4.8	0.75	4.7	0.65
14	86	133	21.3	38	12.7	1.56	10	0.73	7.5	1.47	3.1	0.54	3.81	0.52
15	58	85	10.2	33	5.2	1.16	3.9	0.67	4.6	0.88	2.8	0.45	2.64	0.45
18	48	92	10.4	35	5.3	0.96	3.8	0.67	4.8	0.92	3.0	0.49	2.9	0.46
21	36	65	8.2	27	4.4	0.88	3.0	0.59	4.0	0.88	2.9	0.46	2.9	0.39
22	21	41	9.8	15.8	4.6	0.61	2.1	0.46	3.0	0.74	2.3	0.36	2.4	0.32
23	23	57	8.6	28	4.5	0.91	2.4	0.38	4.5	0.77	1.7	0.34	2.7	0.38
24	19	36	7.6	21	3.3	0.87	3.7	0.49	3.8	0.68	2.1	0.42	2.9	0.44
25	14	46	4.4	17	2.6	0.62	2.1	0.36	3.6	0.61	2.6	0.31	2.1	0.34
35	12	33	4.1	14	2.9	0.67	3.3	0.44	2.8	0.58	1.9	0.36	2.6	0.27

Sample no.	Sc	Co	Ni	Rb	Sr	Y	Zr	Nb	Cs	Ba	Hf	Ta	Th	U
4	25	22	57	124	276	51	193	15.2	5.8	491	5.1	1.3	19.2	2.6
14	24	18	56	133	260	14.6	134	14.2	4.7	542	3.6	1.36	19.4	2.0
15	24	17.9	35	117	136	19.1	285	17.7	6.0	625	7.2	1.04	18.6	3.5
18	18.4	5.8	14.1	131	75	24	227	15.6	5.1	587	5.5	0.93	19.1	2.5
21	17.9	15	23	127	61	28	152	11.7	5.8	496	3.7	0.82	22.5	1.22
22	26	8.7	15.1	124	148	28	258	12.9	5.4	451	7.3	1.43	18.8	2.1
23	18	8.1	18	141	87	27	224	12.7	5.1	570	6.6	1.13	19.2	2.2
24	19	14	21	143	112	29	288	14	4.9	524	7.4	1.22	21.2	2.4
25	21	15.8	34	119	127	24	199	12.2	5.9	498	5.4	0.98	19.4	1.6
35	23	17	22	126	119	30	299	14.4	5.2	533	7.1	1.14	20.1	2.7

Sample no.	$(La/Yb)_n$	$(Gd/Yb)_n$	Eu/Eu*	Ce/Ce*	$(LREE/HREE)_n$	Total REE	La/Sc	Th/Sc	La/Th	Co/Th	Th/U
4	10.57	1.26	0.61	0.92	3.65	335	2.99	0.77	3.88	1.17	7.26
14	15.2	2.11	0.41	0.73	4.56	320.5	3.58	0.81	4.44	0.93	9.55
15	14.75	1.19	0.76	0.78	4.17	209	2.41	0.77	3.11	0.96	5.33
18	11.23	1.05	0.62	0.94	3.87	208.9	2.63	1.04	2.53	0.31	7.55
21	8.42	0.83	0.70	0.88	3.23	157.1	2.03	1.26	1.61	0.67	18.5
22	6.11	0.71	0.52	0.68	3.10	104.6	0.83	0.73	1.13	0.46	9.02
23	5.74	0.72	0.77	0.98	3.34	135.6	1.28	1.07	1.20	0.42	8.73
24	4.42	1.03	0.76	0.72	2.28	102.4	1.00	1.12	0.90	0.66	8.83
25	4.49	0.81	0.79	1.40	2.30	96.64	0.67	0.92	0.72	0.81	12.13
35	3.11	1.02	0.66	1.13	1.89	78.92	0.52	0.87	0.60	0.85	7.44

together with the $(LREE/HREE)_n$ ratio of 1.89–4.56 suggest that the initial sediments were accumulated at the continental margin in a coastal shallow-water setting under humid conditions and tranquil tectonic environment, which facilitated the intense weathering of the rocks. As was mentioned above, this conclusion also follows from the petrochemistry of the rocks and lithofacies data [11].

The conclusions made in this communication are consistent with the Precambrian geological evolution of the Yenisei Ridge: the Late Proterozoic stage of its evolution postdated the continental stage with peneplanation and formation of the weathering crust. The Early–Late Precambrian boundary corresponded to the subplatformal stage with accumulation of high-Al terrigenous and clayey–carbonate sediments of the Teya Group in ensialic rift-type basins due to the erosion of Postarchean granitoid complexes with an age of ~1900 Ma [15]. Relative to Late Proterozoic Fe–Al metapelites at the southwestern framing of the Siberian

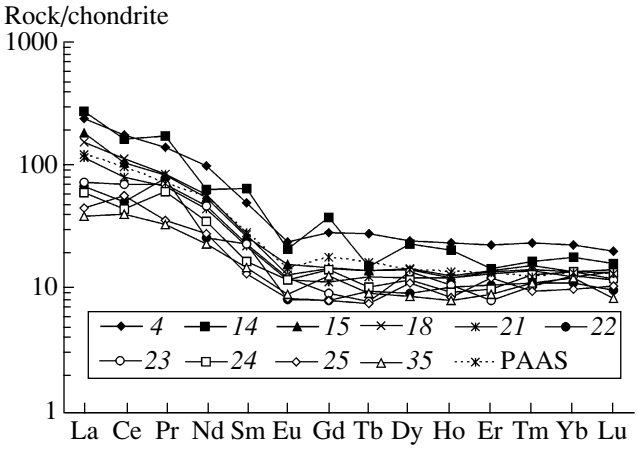

Fig. 3. REE distribution patterns in metapelites of the Teya Group and PASS. Sample numbers (from top to bottom) are located in order of increasing *PT* parameters of metamorphism.

Craton [1, 2], Early Proterozoic metapelites are marked by a high contribution of granitoid material in the erosion zone. The trend of depletion in Th and LREE and enrichment in transition metals with time reflects the Precambrian evolution pattern of the upper continental crust: involvement of the juvenile mafic crust in source areas in the Middle Riphean and Vendian [9, 15].

ACKNOWLEDGMENTS

This work was supported by the Russian Foundation for Basic Research (project no. 06-05-64676), the Foundation of the President of the Russian Federation for the Support of Leading Scientific Schools (project no. NSh-4922.2006.5), and the Siberian Division of the Russian Academy of Sciences (integration project no. 16).

REFERENCES

1. I. I. Likhanov, V. V. Reverdatto, and A. E. Vershinin, Dokl. Earth Sci. **405**, 1186 (2005) [Dokl. Akad. Nauk **404**, 671 (2005)].
2. I. I. Likhanov, V. V. Reverdatto, and A. E. Vershinin, Geol Geofiz. **47** (1), 119 (2006).
3. I. I. Likhanov, V. V. Reverdatto, V. S. Shepelev, et al., Lithos **58**(1/2), 55 (2001).
4. I. I. Likhanov and V. V. Reverdatto, Petrology **13**, 73 (2005), [Petrologiya **13**, 81 (2005)].
5. V. K. Golovenok, *High-Al Complexes of Precambrian*, (Nedra, Leningrad, 1977) [in Russian].
6. Ya. E. Yudovich and M. P. Ketris, *Principles of Lithochemistry* (Nauka, St. Petersburg, 2000) [in Russian].
7. I. I. Likhanov, O. P. Polyansky, V. V. Reverdatto, et al., J. Metamorph. Geol. **22**, 743 (2004).
8. I. I. Likhanov, P. S. Kozlov, V. V. Reverdatto et al., Dokl. Earth Sci. **411**, 1313 (2006) [Dokl. Akad. Nauk **411**, 235 (2006)].
9. S. R. Taylor and S. M. McLennan, *The Continental Crust: Its Composition and Evolution* (Blackwell, Oxford, 1985; Mir, Moscow, 1988).
10. A. A. Predovsky, *Reconstruction of Conditions of Early Precambrian Sedimentogenesis and Volcanism* (Nauka, Leningrad, 1980) [in Russian].
11. E. P. Akul'shina, in *Comparative Analysis of Marine Sedimentation in Precambrian and Paleozoic* (Nauka, Novosibirsk, 1980), pp. 101–125 [in Russian].
12. S. R. Taylor and S. M. McLennan, Rev. Geophys. **33**, 241 (1995).
13. H. Martin, Geology **14**, 753 (1986).
14. J. A. Pearce, Episodes **19**, 120 (1996).
15. A. D. Nozhkin, O. M. Turkina, and V. A. Bobrov, Dokl. Earth Sci. **391**, 718 (2003) [Dokl. Akad. Nauk. **390**, 813 (2003)].